







## Research Article

# The Inhibitory Properties of the Ambroxol Derivative on the Corrosion of Mild Steel in Hydrochloric Acid Medium

Pavel Anatolyevich Nikolaychuk <sup>1</sup>, Aleksandr Igorevich Biryukov <sup>2</sup>,  
Artem Vladimirovich Sharov <sup>1</sup>, Leon Olegovich Burmistrov <sup>2</sup>,  
Natalya Sergeevna Amelina <sup>2</sup> and Anastasia Andreevna Tereshkina <sup>1</sup>

<sup>1</sup>Laboratory of Advanced Materials for Industry and Biomedicine, Kurgan State University, Kurgan, Russia

<sup>2</sup>Department of Analytical and Physical Chemistry, Chelyabinsk State University, Chelyabinsk, Russia

Correspondence should be addressed to Artem Vladimirovich Sharov; sharow84@gmail.com

Received 9 August 2023; Revised 23 November 2023; Accepted 2 January 2024; Published 29 January 2024

Academic Editor: Manikandan M

Copyright © 2024 Pavel Anatolyevich Nikolaychuk et al. This is an open access article distributed under the Creative Commons Attribution License, which permits unrestricted use, distribution, and reproduction in any medium, provided the original work is properly cited.

A compound 2-(6,8-dibromo-3-(4-hydroxycyclohexyl)-1,2,3,4-tetrahydroquinazolin-2-yl)phenol was synthesised from ambroxol hydrochloride and salicylaldehyde. The structure of the compound was studied with UV, IR, Raman, and <sup>1</sup>H NMR spectroscopy. The inhibitory ability of the synthesised compound on the corrosion of mild stainless steel EN Fe37-3FN in 0.5 M hydrochloric acid solution was studied using gravimetric and electrochemical methods, including potentiodynamic polarisation and EIS. It was shown that the inhibitory activity of the compound increases with the increase of its concentration in a solution. An addition of 3 mg/l of the compound reduces the corrosion rate by 20% and that of 400 mg/l by 85%. The data of gravimetric and electrochemical measurements coincide well. The sorption of the compound on the metal surface obeys the Langmuir adsorption isotherm, and the nature of adsorption is physical. The compound exhibits the chelating activity with both ferrous and ferric ions in the acidic solution. The synthesised compound may be a good choice for the inhibition of steel corrosion in acidic environments.

## 1. Introduction

Various compounds belonging to the different classes of organic compounds demonstrate the ability to slow the oxidation of metals in aqueous environments [1]. The usage of expired drugs as the corrosion inhibitors [2–4] is a prospective and fast-growing research field around the world. One of the active pharmaceutical ingredients, in which inhibitory activity on the corrosion of stainless steel in the acidic medium was already demonstrated [5–7], is ambroxol. Moreover, it was already shown [8, 9] that the chemical modification of different pharmaceuticals might improve their inhibitory properties, and the usage of derivatised pharmaceutical ingredients is also a prominent research field. In the literature, there are several pieces of evidence [10] that the products of condensation of aromatic primary amines with aromatic aldehydes exhibit excellent inhibitory

properties. Recently, a synthesis of the new derivative of ambroxol and salicylaldehyde [11], namely, 2-(6,8-dibromo-3-(4-hydroxycyclohexyl)-1,2,3,4-tetrahydroquinazolin-2-yl)phenol (Figure 1), was reported. The toxicity of the reported compound was also estimated [11] using the ProTox-II web application [12], and it was found that the compound is nontoxic, with the predicted LD<sub>50</sub> equal to 12 g/kg. In the present study, the aim is to investigate the inhibitory properties of this compound on the corrosion of mild stainless steel EN Fe37-3FN in 0.5 M hydrochloric acid medium.

## 2. Reagents and Equipment

Ambroxol hydrochloride was kindly provided as a gift by Velpharm LLC (Kurgan). Salicylaldehyde (analytical grade), ethanol (analytical grade), methanol (analytical grade),

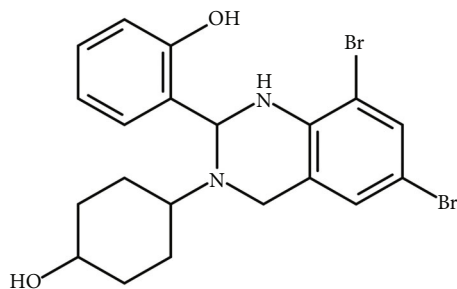


FIGURE 1: A structural formula of 2-(6,8-dibromo-3-(4-hydroxycyclohexyl)-1,2,3,4-tetrahydroquinazolin-2-yl)phenol [11].

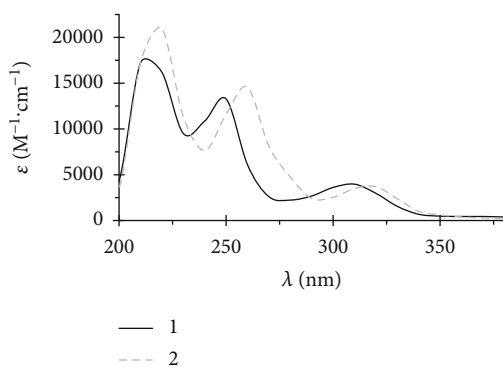


FIGURE 2: The UV spectra of 1: ambroxol hydrochloride and 2: 2-(6,8-dibromo-3-(4-hydroxycyclohexyl)-1,2,3,4-tetrahydroquinazolin-2-yl)phenol in methanol.

propan-2-ol (analytical grade), and sodium carbonate (analytical grade) were purchased from Chimmed LLC. Hydrochloric acid (pure grade) and potassium bromide (spectroscopic grade) were purchased from Vekton LLC. Ferric chloride (analytical grade) and Mohr salt (analytical grade) were purchased from Lenreaktiv LLC. In addition, salicylaldehyde was redistilled, and potassium bromide was dried prior to use. Steel electrodes were manufactured from rectangular ingots made of mild stainless steel EN Fe37-3FN (containing no more than 0.14% C; 0.3% Ni, Cu, and Cr; 0.05% Si; 0.4% Mn; 0.05% P; and 0.04% S) with the dimension  $2 \times 2$  mm, the unused surface was sealed by epoxy resin, and the surface area of the flat working surface immersed in the solution was  $0.04 \text{ cm}^2$ . For gravimetric measurements, rectangular flat plates from the same steel with the thickness of 3 mm, width of  $20 \pm 2$  mm, and height of  $30 \pm 2$  mm were used.

Weighting of the samples was performed using the analytical balances AND GR20 and VL-324. The UV spectra of ambroxol hydrochloride and ambroxol derivative (AD) were recorded from the methanolic solutions of the respective components with the concentration of 1 mM and from the solutions in 0.5M HCl with the concentration of  $40 \mu\text{M}$  using the spectrometer Specol 1200 in a quartz cuvette with the optical path length of 1 cm in the wavelength range from 190 to 400 nm with the step of 2 nm. The IR spectra of ambroxol hydrochloride, ambroxol free base, and ambroxol derivative were recorded from the tablets with potassium

bromide using the spectrometers FT-801 and Shimadzu IRAffinity 1S with the resolution of  $4 \text{ cm}^{-1}$ , number of scans equal to 32, and the wavenumber range from 500 to  $4000 \text{ cm}^{-1}$ . The Raman spectrum of the ambroxol derivative was recorded using the portative spectrometer InSpektr R532 equipped with the laser with the wavelength of 532 nm, with the resolution of  $6 \text{ cm}^{-1}$ , and the wavenumber range from 140 to  $4000 \text{ cm}^{-1}$ . The  $^1\text{H}$  NMR spectrum of the ambroxol derivative in methanol- $d_4$  was recorded using the spectrometer Bruker Avance-AV 400, with the frequency of 400.13 MHz. Electrochemical measurements were conducted using the potentiostat-galvanostat P-40X and the EIS measurements using the potentiostat-galvanostat P-45X with the frequency response analyser FRA-24M. The distilled water for solution preparation was produced using the aquadistillers LISTON A1204 and AE-10. The magnetic stirrer US-6120 was used for stirring. A laboratory glassware of 2nd grade was used.

### 3. Liberation of Ambroxol Free Base from Ambroxol Hydrochloride

A total of 800 mg of ambroxol hydrochloride was dissolved in 200 ml of distilled water. A total of 200 mg of sodium carbonate was dissolved in 18 ml of distilled water. The solution of sodium carbonate was gently added as a very thin stream to the solution of ambroxol hydrochloride while stirring, and the solution was left stirred for 60 min. A precipitate of the ambroxol free base was washed by distilled water several times, filtered, and dried *in vacuo*. The yield was 495 mg (72%).

### 4. Synthesis of 2-(6,8-Dibromo-3-(4-hydroxycyclohexyl)-1,2,3,4-tetrahydroquinazolin-2-yl)phenol

A total of 341 mg (1.0 mmol) of ambroxol free base and of 122 mg (1.0 mmol) of salicylaldehyde were dissolved in ethanol, the solutions were mixed together, and the mixture was boiled under the reflux condenser over 4 h and then cooled. The precipitate was recrystallised from ethanol and dried *in vacuo*. The crystalline dry solid product was white, and its solution in ethanol was yellow. The yield was 303 mg (68%).

### 5. Characterisation of the Obtained Compound

In order to confirm the structure of the synthesised compound, its UV, IR, Raman, and  $^1\text{H}$  NMR spectra were recorded.

The UV spectra are presented in Figure 2.

The absorption bands on the UV spectrum of the derivative exhibit a clear bathochromic shift compared with those on the spectrum of ambroxol. The first two bands also exhibit a hyperchromic shift, whereas the third band exhibits a slight hypochromic shift. The absorption maxima coincide with those presented in the literature (214, 244, and 308 nm for ambroxol hydrochloride [13] and 216, 256, and 316 nm for ambroxol derivative [11]).

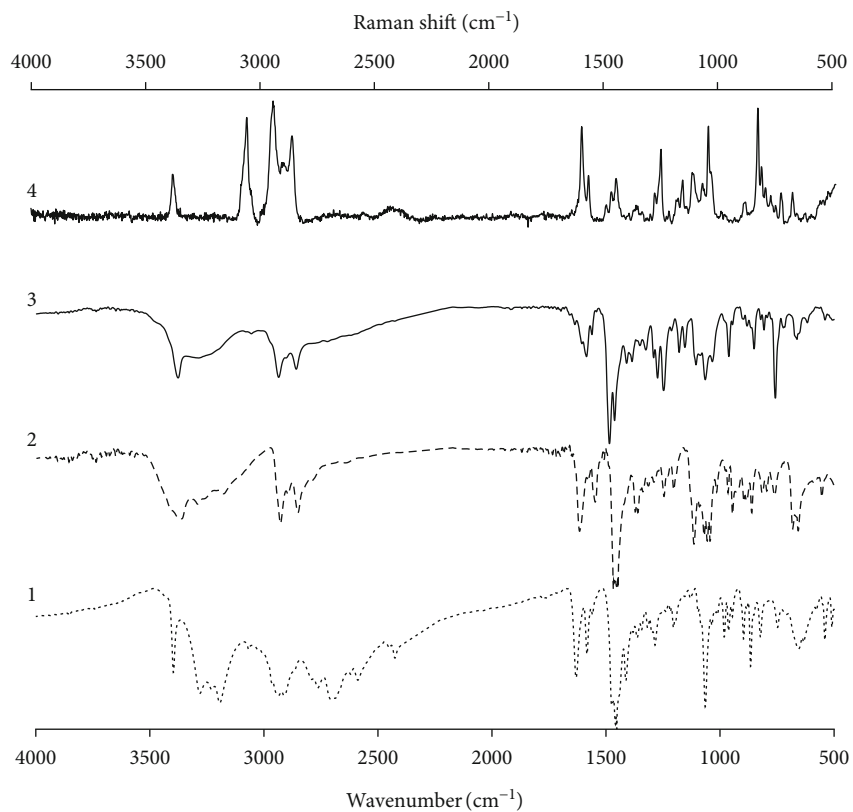


FIGURE 3: The IR and Raman spectra: 1: IR spectrum of ambroxol hydrochloride; 2: IR spectrum of ambroxol free base; 3: IR spectrum of 2-(6,8-dibromo-3-(4-hydroxycyclohexyl)-1,2,3,4-tetrahydroquinazolin-2-yl)phenol; 4: Raman spectrum of 2-(6,8-dibromo-3-(4-hydroxycyclohexyl)-1,2,3,4-tetrahydroquinazolin-2-yl)phenol.

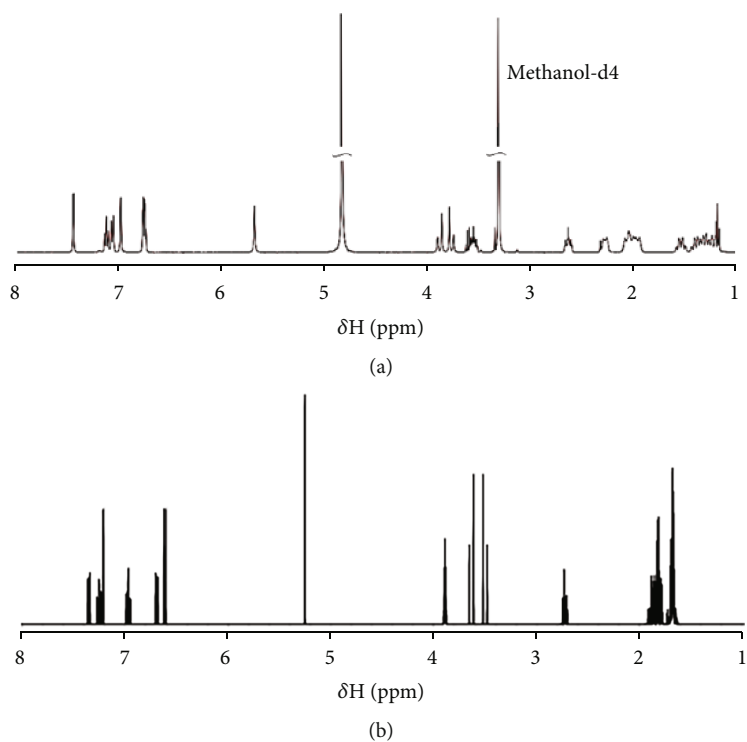


FIGURE 4: <sup>1</sup>H NMR spectrum of 2-(6,8-dibromo-3-(4-hydroxycyclohexyl)-1,2,3,4-tetrahydroquinazolin-2-yl)phenol: (a) experimental; (b) predicted.

The IR and Raman spectra are presented in Figure 3.

The bands in the wavenumber range from 3080 to 3500  $\text{cm}^{-1}$  in the spectra of the ambroxol derivative corresponding to the vibrations of the OH and NH groups. In the range from 2800 to 3090  $\text{cm}^{-1}$ , there are bands corresponding to the vibrations of the C–H bonds in aromatic rings and at the saturated carbon atoms. In the “fingerprint” range from 1460 to 1700  $\text{cm}^{-1}$ , there are bands corresponding to the vibrations of C=C, NH (1535–1700), OH (1482), and NH (1460) bonds [11]. The similar bands, taking into account the intensity change of the symmetric and asymmetric vibrations, are present at the Raman spectrum of the ambroxol derivative (4 in Figure 3). The differences that are revealed in the spectra 1, 2, and 3 (Figure 3) in the ranges 3080–3500  $\text{cm}^{-1}$  and 1460–1700  $\text{cm}^{-1}$  are due to the disappearance of the protonated forms of the amine nitrogen in the ambroxol free base and due to the transition of the primary and secondary amino groups in free ambroxol into the secondary and tertiary ones in the ambroxol derivative.

In addition to the experimentally recorded  $^1\text{H}$  NMR spectrum (Figure 4(a)), a modelled spectrum (Figure 4(b)) predicted by the tool <http://nmrdb.org/> [14] was obtained.

The recorded UV and IR spectra of the ambroxol derivative coincide with those from the study [11]. Moreover, the position and multiplicity of the bands in the experimental and predicted [14] NMR spectra also generally coincide. Therefore, the spectroscopic results certainly prove that the synthesised compound is exactly the 2-(6,8-dibromo-3-(4-hydroxycyclohexyl)-1,2,3,4-tetrahydroquinazolin-2-yl)phenol.

## 6. Gravimetric Studies

For gravimetric tests, solutions of 0.5 M hydrochloric acid and 0.5 M hydrochloric acid with the different additions of ambroxol derivative ranging from 3 to 400 ppm were prepared. Rectangular flat plates made of EN Fe37-3FN mild stainless steel with thickness of 3 mm, width of  $20 \pm 2$  mm, and height of  $30 \pm 2$  mm were polished using the P2500 emery paper and degreased by propan-2-ol. The weighted plates ( $m_0$ , mg) were immersed into corrosive media for 2 h, then washed with distilled water, dried, and reweighted ( $m$ , mg). Each experiment was performed in triplicate. From the measured weight losses ( $\Delta m = m_0 - m$ , mg), sample surfaces ( $S$ ,  $\text{cm}^2$ ), and immersion times ( $t$ , h), the average corrosion rates ( $\omega$ ,  $\text{mg}/(\text{cm}^2 \cdot \text{h})$ ) were estimated:

$$\omega = \frac{\Delta m}{S \cdot t}. \quad (1)$$

An inhibitory ability ( $\eta$ , %) of the compound was estimated from the ratio of the corrosion rates in the absence ( $\omega_0$ ) and in the presence ( $\omega$ ) of the inhibitor [15]:

$$\eta = \frac{\omega_0 - \omega}{\omega_0} \cdot 100\%. \quad (2)$$

TABLE 1: The results of the gravimetric measurement of the corrosion rates.

$c_{\text{inh}}$ (ppm)	$\omega$ ( $\text{mg}/(\text{cm}^2 \cdot \text{h})$ )	$\eta$ (%)
0	$0.78 \pm 0.08$	—
3.2	$0.67 \pm 0.06$	19.6
16	$0.43 \pm 0.05$	44.8
80	$0.27 \pm 0.04$	65.3
400	$0.13 \pm 0.03$	82.7

The dependence of the measured inhibition efficiencies at the different inhibitor concentrations ( $c_{\text{inh}}$ , ppm) is presented in Table 1.

## 7. Polarisation Studies

For polarisation tests, solutions of 0.5 M hydrochloric acid and 0.5 M hydrochloric acid with the different additions of the ambroxol derivative ranging from 3 to 400 ppm were prepared. Electrodes made of EN Fe37-3FN mild stainless steel and sealed with the epoxy resin with the working surface of 4  $\text{mm}^2$  were polished using the P2500 emery paper and felt cloth and degreased by propan-2-ol. The measurements were conducted using the potentiostat-galvanostat P-40X in a standard three-electrode electrochemical cell, consisting from the working electrode (steel sample), auxiliary graphite electrode, and silver-silver chloride reference electrode. An open circuit potential ( $E_{\text{corr}}$ , mV) was recorded during 30 min. Polarisation curves were recorded in the potential range from  $-500$  to  $+500$  mV relatively to the measured open circuit potential with the potential sweep rate of 10 mV/s. Each experiment was performed in triplicate. The obtained polarisation curves were presented in the coordinates  $E(\lg i)$ , and the Tafel slopes of the anodic ( $b_a$ , mV/dec) and cathodic ( $b_c$ , mV/dec) branches of the polarisation curves, the corrosion current densities ( $i_{\text{corr}}$ ,  $\text{A}/\text{cm}^2$ ), and the polarisation resistances ( $R_p$ ,  $\text{ohm} \cdot \text{cm}^2$ ) were evaluated from them using the Stern – Geary equation [15]:

$$R_p = \frac{1}{\ln 10} \cdot \frac{1}{i_{\text{corr}}} \cdot \frac{b_a \cdot |b_c|}{b_a + |b_c|}. \quad (3)$$

The inhibitory ability of the compound was estimated either from the ratio of the corrosion current densities in the absence ( $i_{\text{corr},0}$ ) and in the presence ( $i_{\text{corr}}$ ) of the inhibitor:

$$\eta = \frac{i_{\text{corr},0} - i_{\text{corr}}}{i_{\text{corr},0}} \cdot 100\%, \quad (4)$$

or from the ratio of the polarisation resistances ( $R_{p,0}$ ,  $R_p$ ) [15]:

$$\eta = \frac{R_p - R_{p,0}}{R_p} \cdot 100\%. \quad (5)$$

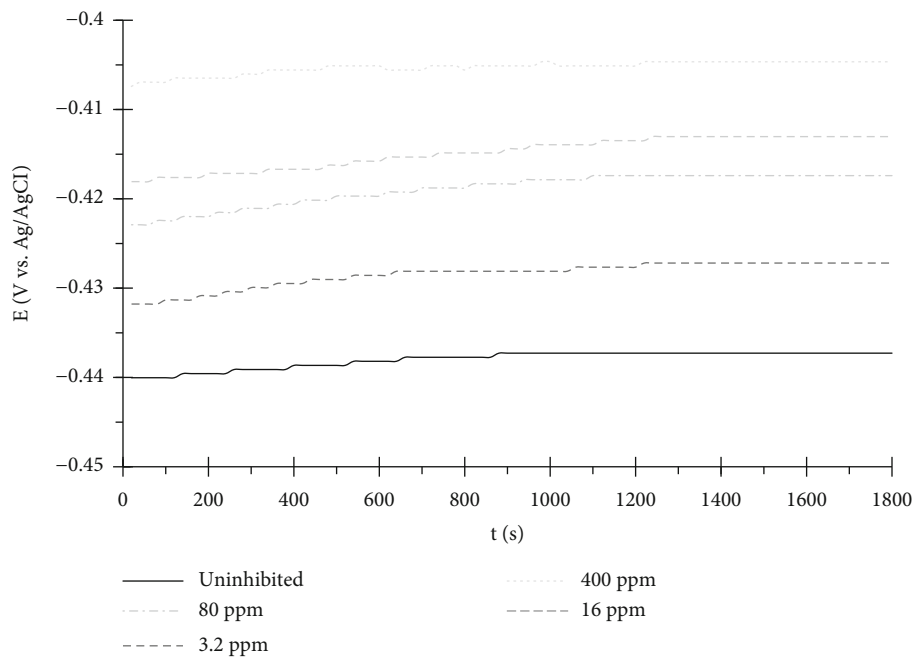


FIGURE 5: The open circuit potential of steel in 0.5 M HCl with the different additions of inhibitor after 30 min of exposure.

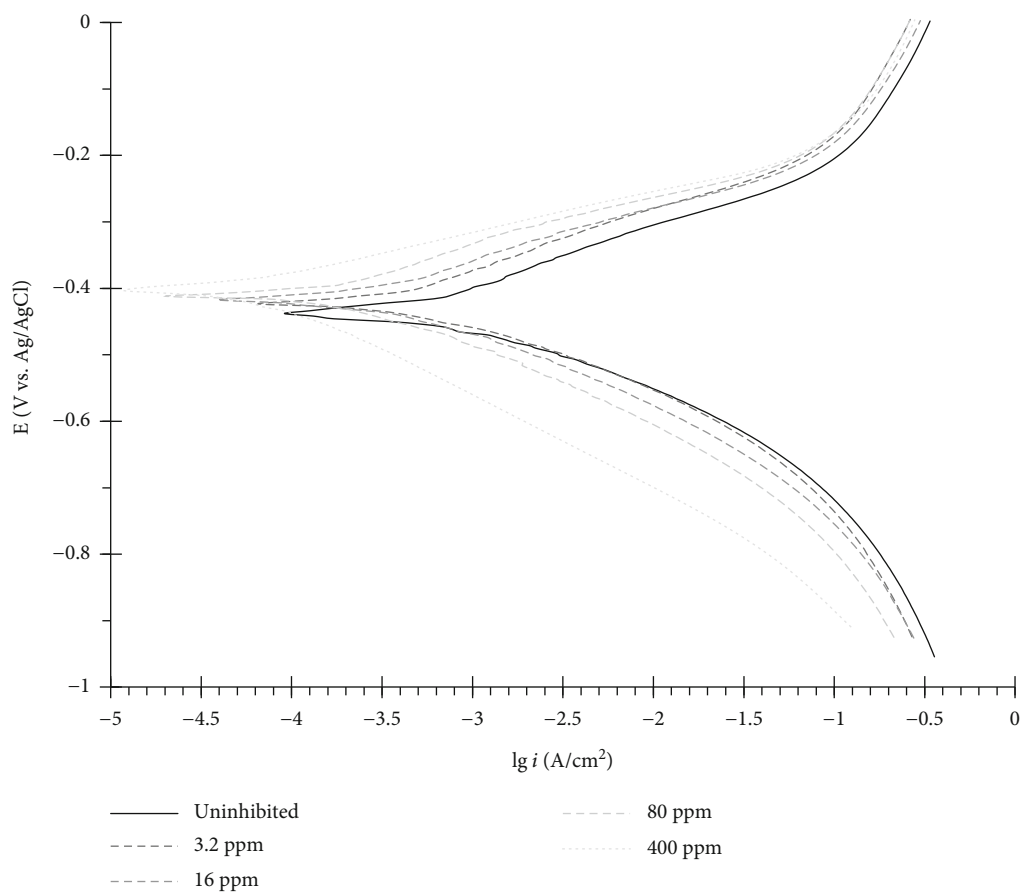


FIGURE 6: The potentiodynamic polarisation curves of steel in 0.5 M HCl with the different additions of inhibitor.

TABLE 2: The results of the electrochemical measurement of the corrosion rates.

$c_{inh}$ (ppm)	$E_{corr}$ (mV)	$b_a$ (mV/dec)	$b_c$ (mV/dec)	$R_p$ (ohm·cm <sup>2</sup> )	$\eta$ (%)	$i_{corr}$ (mA/cm <sup>2</sup> )	$\eta$ (%)
0	-437	85.4	-119.2	187	—	0.611	—
3.2	-424	84.5	-126.0	240	21.7	0.486	20.5
16	-417	76.2	-128.6	334	43.8	0.330	46.0
80	-412	67.8	-136.9	535	65.0	0.195	68.0
400	-404	61.5	-144.3	1504	87.5	0.066	89.2

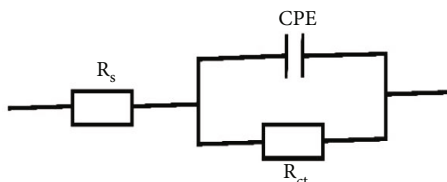


FIGURE 7: The simplified Randles equivalent electrical circuit.

The results are presented in Figures 5 and 6 and in Table 2.

## 8. EIS Studies

For EIS tests, the solutions of 0.5 M hydrochloric acid and 0.5 M hydrochloric acid with the different additions of the ambroxol derivative ranging from 3 to 400 ppm were prepared. Electrodes made of EN Fe37-3FN mild stainless steel and sealed with epoxy resin with the working surface of 4 mm<sup>2</sup> were polished using the P2500 emery paper and degreased by ethanol. The measurements were conducted using the potentiostat-galvanostat P-45X equipped with the frequency response analyser FRA-24M in a standard three-electrode electrochemical cell, consisting from the working electrode (steel sample), auxiliary electrode from the porous graphite, and silver-silver chloride reference electrode. The electrochemical cell was placed into the Faraday shield cell SH-3M. An open circuit potential was recorded during 30 min. Impedance values were recorded at the open circuit potential value in the alternate current frequency interval from 100 mHz to 10 kHz with the potential amplitude of 10 mV. Each experiment was performed in triplicate. The obtained results were presented in the form of Bode and Nyquist plots [15]. For the estimation of the impedance parameters, a simplified Randles equivalent electrical circuit [16] (Figure 7), containing the solution resistance ( $R_s$ , ohm), the consecutive charge transfer resistance ( $R_{ct}$ , ohm) of the passivation layer, and the parallel constant-phase element representing the double electric layer, was employed.

The impedance of this circuit is expressed by the following equation:

$$Z = R_s + \frac{1}{1/R_{ct} + P \cdot (i \cdot \omega)^n}$$

$$= R_p + \frac{1}{1/R_{ct} + P \cdot \omega^n \cdot (\cos((\pi \cdot n)/2) + i \cdot \sin((\pi \cdot n)/2))}, \quad (6)$$

where  $\omega$ (Hz) is the frequency of the alternate current and  $P$  (ohm<sup>-1</sup>·s<sup>n</sup>) and  $n$  are the parameters of the constant phase element.

The fitting of the equivalent circuit parameters to the experimental impedance values was performed using the free software EIS Spectrum Analyser [17].

In addition, the capacitance ( $C_{dl}$ , F) and the thickness ( $d$ , m) of the double electric layer on the metal-solution interface were estimated [18]:

$$C_{dl} = \frac{1}{2\pi \cdot R_{ct} \cdot \omega_{max}}, \quad (7)$$

$$d = \frac{\epsilon \cdot \epsilon_0 \cdot S}{C_{dl}},$$

where  $\omega_{max}$  (Hz) is the frequency of the alternate current that corresponds to the maximum at the Nyquist plot and  $S$  (m<sup>2</sup>) is the electrode surface.

The inhibitory ability of the compound was estimated from the ratio of the charge transfer resistances in the presence ( $R_{ct}$ ) and in the absence ( $R_{ct,0}$ ) of the inhibitor [15]:

$$\eta = \frac{R_{ct} - R_{ct,0}}{R_{ct}} \cdot 100\%. \quad (8)$$

The results are presented in Figures 8 and 9 and in Table 3.

## 9. Langmuir Adsorption Model

The description of the adsorption of the inhibitor on the steel surface was performed in terms of the Langmuir adsorption model. The Langmuir adsorption isotherm equation was linearised in the following form:

$$\frac{c_{inh}}{\eta} = \frac{1}{K_{ads}} + c_{inh}, \quad (9)$$

where  $c_{inh}$  is the concentration of the inhibitor (ppm),  $K_{ads}$  is the adsorption-desorption equilibrium constant, and  $\eta$  is the percentage of the surface covered by the inhibitor, which is assumed to be equal to the inhibition efficiency. The dependencies of  $c_{inh}/\eta$  on  $c_{inh}$  are presented in Figure 10 and in Table 4. The data were processed using the least squares technique, and the equilibrium constants  $K_{ads}$  were estimated as the intercepts of the regression equations. The

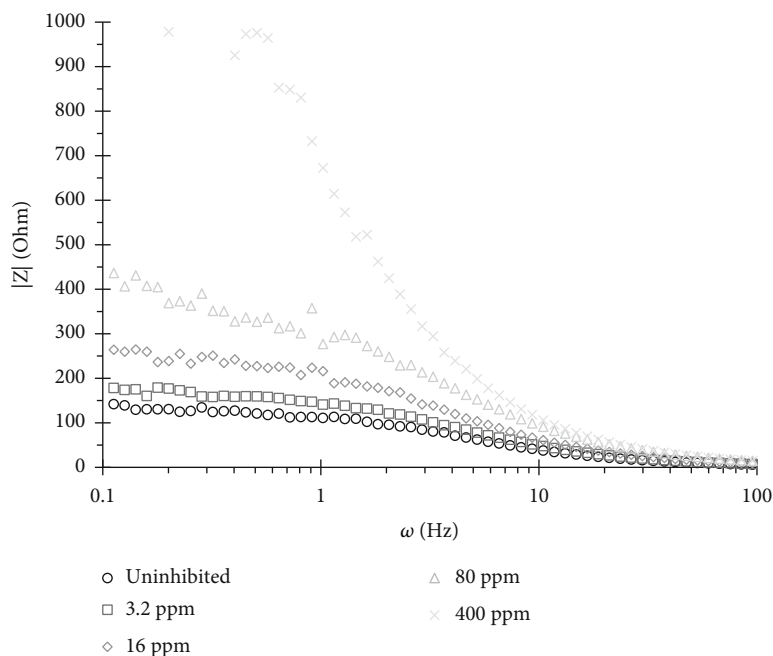


FIGURE 8: The Bode plot of steel in 0.5 M HCl with the different additions of inhibitor.

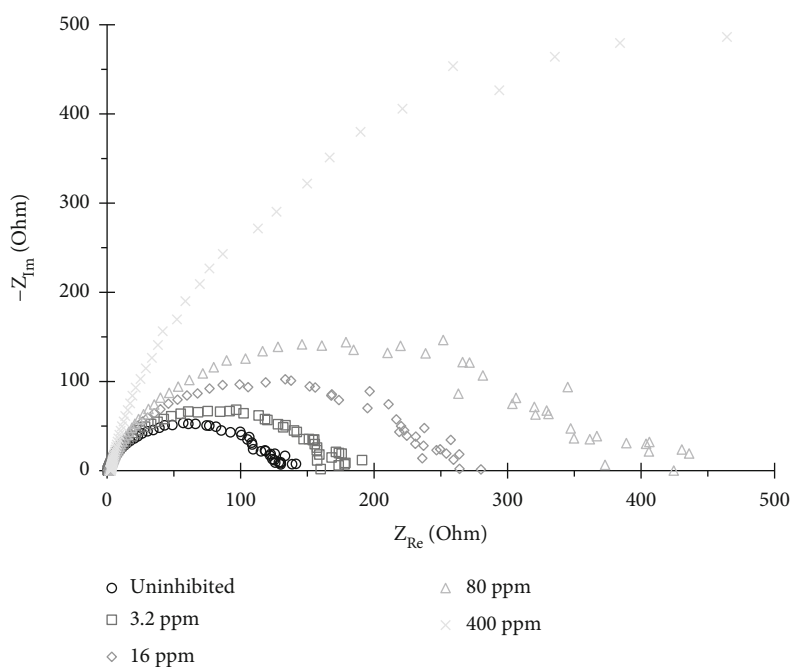


FIGURE 9: The Nyquist plot of steel in 0.5 M HCl with the different additions of inhibitor.

Gibbs energy changes of the sorption were estimated from the following equation:

$$\Delta_{\text{ads}}G = -R \cdot T \cdot \ln (K_{\text{ads}} \cdot c_{\text{water}}), \quad (10)$$

where  $c_{\text{water}} = 10^6$  ppm is the water concentration in the extracts. The results are presented in Table 4.

### 10. Chelating Ability of Ambroxol Derivative with Iron

In order to study the chelating ability of the synthesised AD with iron in the acidic solution, the UV spectra of the  $40 \mu\text{M}$  AD and the equimolar mixtures of  $40 \mu\text{M}$  AD +  $40 \mu\text{M}$  ferric chloride and  $40 \mu\text{M}$  AD +  $40 \mu\text{M}$  Mohr salt solutions in 0.5 M HCl after 24 h of exposure were recorded. The spectra are presented in Figures 11 and 12.

TABLE 3: The results of the EIS measurement of the corrosion rates.

$c_{inh}$ (ppm)	$R_s$ (ohm)	Constant phase element parameters				$R_{ct}$ (ohm)	$\eta$ (%)
		$P$ (kohm <sup>-1</sup> ·s <sup>n</sup> )	$n$	$C_{dl}$ ( $\mu$ F)	$d$ (pm)		
0	0.61	0.49	0.88	333	8.5	130	—
3.2	0.58	0.54	0.88	240	11.8	160	18.9
16	0.62	0.55	0.89	227	12.5	215	39.3
80	0.59	0.57	0.87	171	16.6	359	63.8
400	0.63	0.85	0.92	116	24.6	844	84.6

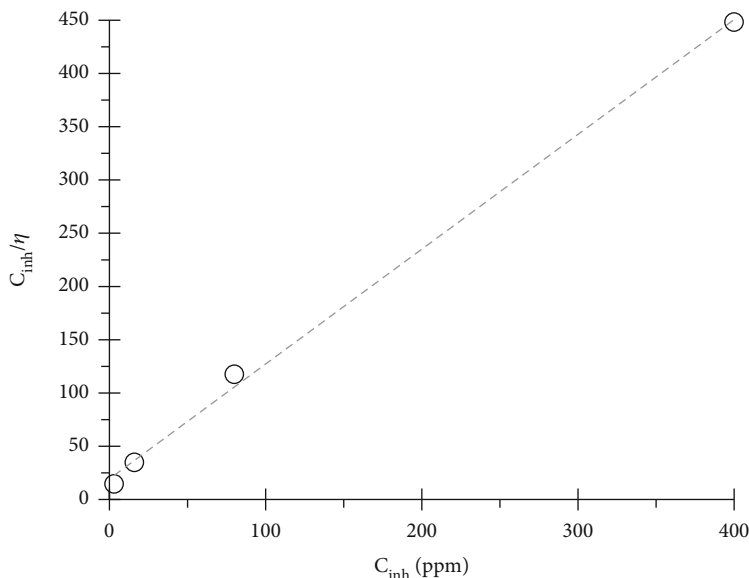
FIGURE 10: The plot of  $c_{inh}/\eta$  vs.  $c_{inh}$  for the adsorption of the inhibitor on the steel surface.

TABLE 4: The parameters of the Langmuir adsorption model.

$C_{inh}$ (ppm)	$\eta$	$C_{inh}/\eta$	Regression equation	$K_{ads}$	$\Delta_{ads}G$ (kJ/mol)
3.2	0.205	14.7	$c_{inh}/\eta = (1.08 \pm 0.03) \cdot c_{inh} + (19 \pm 7)$ $R^2 = 0.998$	$0.05 \pm 0.02$	$-27 \pm 1$
16	0.460	34.8			
80	0.680	117.6			
400	0.892	448.4			

The presented spectra show that in the presence of ferric ions, the band of AD at 214 nm disappears, the bands at 248 and 312 nm exhibit the slight hypsochromic and clear hyperchromic shifts, and the shoulder at 344 nm appears. In the presence of ferrous ions, both the bands at 214 and 248 nm disappear, and the shoulder at 338 nm appears. This suggests that the ambroxol derivative forms the complexes with both ferrous and ferric ions in the acidic solution.

## 11. Discussion

The results of the gravimetric, electrochemical, and EIS measurements coincide well. They show that the inhibitory activity of the ambroxol derivative against the corrosion of mild stainless steel EN Fe37-3FN in a 0.5 M hydrochloric

medium depends on the inhibitor concentration in the solution. Even the addition of 3 mg of the ambroxol derivative compound to each litre of solution provides the inhibition efficiency of ~20%, whereas the addition of 80 mg of the compound to each litre of solution provides an ~65% inhibition efficiency, and at the concentration of 400 mg/l, the inhibition efficiency rises to ~85%.

The adsorption of the inhibitor at the steel surface fairly obeys the Langmuir adsorption model. The Gibbs energy of sorption equals  $-27$  kJ/mol, which means that the nature of the sorption is physical due to the electrostatic interactions [19].

The UV spectra of the inhibitor and its mixtures with both ferrous and ferric ions differ significantly, which means that the studied compound forms chelates with these ions in acidic environments.



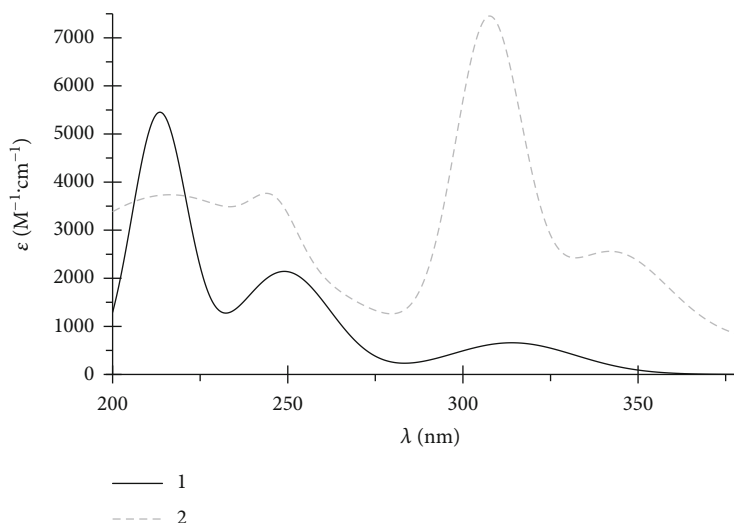


FIGURE 11: The UV spectra of 1: ambroxol derivative in 0.5 M HCl and 2: equimolar mixture of AD + ferric chloride in 0.5 M HCl.

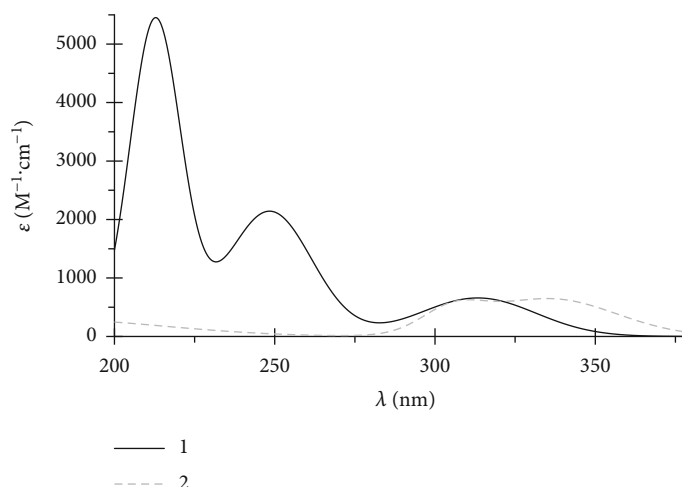


FIGURE 12: The UV spectra of 1: ambroxol derivative in 0.5 M HCl and 2: equimolar mixture of AD + Mohr salt in 0.5 M HCl.

The inhibition mechanism might be linked with the displacement of the water molecules adsorbed on the steel surface by the inhibitor molecules and the formation of the protective film. In addition, the inhibitor in the solution forms complex compounds with the formed ferrous or ferric ions, which shifts the corrosion potentials to the more positive values.

In the studies [5–7], the inhibitory action of ambroxol hydrochloride on the corrosion of mild steel in 1 M hydrochloric [5, 6] and 1 M sulphuric acids [6, 7] was studied. From the gravimetric and electrochemical tests, it was shown there that the additions of ambroxol hydrochloride at the concentration levels from 1 to 9% (from 10 to 90 g/l) slow the corrosion processes down to 50–90%.

Therefore, the implementation of the ambroxol derivative allows to achieve the comparable values of inhibition efficiencies with those of underivatized ambroxol, but using the 30–40 times less concentrated inhibitor solution. This confirms the fact [8] that the chemical modification of pharmaceuticals

improves their inhibitory properties. The availability of the source reagents (ambroxol and salicylaldehyde) and the simple synthesis protocol make the compound 2-(6,8-dibromo-3-(4-hydroxycyclohexyl)-1,2,3,4-tetrahydroquinazolin-2-yl)phenol a prospective corrosion inhibitor for industrial use.

## 12. Conclusion

A synthesis of the compound 2-(6,8-dibromo-3-(4-hydroxycyclohexyl)-1,2,3,4-tetrahydroquinazolin-2-yl)phenol from ambroxol hydrochloride and salicylaldehyde was performed. The structure of the obtained compound was investigated using UV, IR, Raman, and  $^1\text{H}$  NMR spectroscopy, and the consistency of the obtained spectra with the literature data is confirmed.

The inhibitory ability of the synthesised compound on the corrosion of mild stainless steel EN Fe37-3FN in 0.5 M hydrochloric acid medium was investigated using gravimetric and electrochemical methods, as well as EIS. It was shown that

the addition of 3 mg/l of the compound reduces the corrosion rate by 20% and the addition of 400 mg/l by 85%. From the literature data, the similar inhibition efficiency using the underivatized ambroxol could only be achieved by using 30-40-fold inhibitor concentrations. This makes the 2-(6,8-dibromo-3-(4-hydroxycyclohexyl)-1,2,3,4-tetrahydroquinazolin-2-yl)phenol a prospective compound for reducing the steel corrosion rate in acidic environments.

## Data Availability

All data are present within the article.

## Conflicts of Interest

The authors declare that they have no conflicts of interest.

## Acknowledgments

The authors are very grateful to Velpharm LLC (Kurgan) for kindly providing the ambroxol hydrochloride as a gift. This work was supported by the state assignment of the Ministry of Science and Higher Education of the Russian Federation (Project Reg. No. 720000Ф.99.1.БН60АА13000) and by the Funding of Perspective Scientific Researches of Chelyabinsk State University.

## References

- [1] R. Aslam, G. Serdaroglu, S. Zehra et al., "Corrosion inhibition of steel using different families of organic compounds: past and present progress," *Journal of Molecular Liquids*, vol. 348, article 118373, 2022.
- [2] N. Vaszilcsin, D. A. Duca, A. Flueraş, and M. L. DANa, "Expired drugs as inhibitors in electrochemical processes—a mini-review," *Studia Universitatis Babeş-Bolyai Chimia*, vol. 64, no. 3, pp. 17–32, 2019.
- [3] G. K. Shamnamol, K. P. Sreelakshmi, G. Ajith, and J. M. Jacob, "Effective utilization of drugs as green corrosion inhibitor—a review," *AIP Conference Proceedings*, vol. 2225, no. 1, article 070006, 2020.
- [4] M. J. Baari and C. W. Sabandar, "A review on expired drug-based corrosion inhibitors: chemical composition, structural effects, inhibition mechanism, current challenges, and future prospects," *Indonesian Journal of Chemistry*, vol. 21, no. 5, pp. 1316–1336, 2021.
- [5] P. Geethamani, M. Narmatha, R. Dhanalakshmi, S. Aejitha, and P. K. Kasthuri, "Corrosion inhibition and adsorption properties of mild steel in 1 M hydrochloric acid medium by expired ambroxol drug," *Journal of Bio- and Tribo-Corrosion*, vol. 5, no. 1, article 16, 2019.
- [6] P. Geethamani and P. K. Kasthuri, "Adsorption and corrosion inhibition of mild steel in acidic media by expired pharmaceutical drug," *Cogent Chemistry*, vol. 1, no. 1, article 1091558, 2015.
- [7] P. Geethamani, P. K. Kasthuri, and A. Aejitha, "Corrosion inhibition of mild steel in sulphuric acid medium by ambroxol drug," *Journal of Applied Chemical Science International*, vol. 3, no. 4, pp. 151–157, 2015.
- [8] M. R. Al-Hadeethi, H. Lgaz, A. Chaouiki, R. Salghi, and H. S. Lee, "Chemical medicines as corrosion inhibitors," in *Organic Corrosion Inhibitors: Synthesis, Characterization, Mechanism, and Applications*, C. Verma, Ed., pp. 287–314, Wiley, New York, 2021.
- [9] P. Singh, D. S. Chauhan, S. S. Chauhan, G. Singh, and M. A. Quraishi, "Chemically modified expired dapsone drug as environmentally benign corrosion inhibitor for mild steel in sulphuric acid useful for industrial pickling process," *Journal of Molecular Liquids*, vol. 286, article 110903, 2019.
- [10] A. Singh and M. A. Quraishi, "Acidizing corrosion inhibitors: a review," *Journal of Materials and Environmental Science*, vol. 6, no. 1, pp. 224–235, 2015.
- [11] A. I. Kryszantiewa, J. K. Voronina, and D. A. Safin, "A novel ambroxol-derived tetrahydroquinazoline with a potency against SARS-CoV-2 proteins," *International Journal of Molecular Sciences*, vol. 24, no. 5, article 4660, 2023.
- [12] P. Banerjee, A. O. Eckert, A. K. Schrey, and R. Preissner, "Pro-Tox-II: a webserver for the prediction of toxicity of chemicals," *Nucleic Acids Research*, vol. 46, no. W1, pp. w257–w263, 2018.
- [13] S. Deepak, "Spectrophotometric method development and validation for simultaneous estimation of salbutamol sulphate and ambroxol hydrochloride in combined dosage forms," *International Journal of Drug Development and Research*, vol. 5, no. 4, pp. 124–132, 2013.
- [14] D. Banfi and L. Patiny, "www.nmrdb.org: resurrecting and processing NMR spectra on-line," *Chimia*, vol. 62, no. 4, pp. 280–281, 2008.
- [15] A. Kadhim, A. A. Al-Amiery, R. Alazawi, M. K. Al-Ghezi, and R. H. Abass, "Corrosion inhibitors. A review," *International Journal of Corrosion and Scale Inhibition*, vol. 10, no. 1, pp. 54–67, 2021.
- [16] X. Z. Yuan, C. Song, H. Wang, and J. Zhang, "EIS equivalent circuits," in *Electrochemical Impedance Spectroscopy in PEM Fuel Cells: Fundamentals and Applications*, X. Z. Yuan, Ed., pp. 139–192, Springer, Berlin, 2010.
- [17] A. S. Bondarenko and G. A. Ragoisha, "Inverse problem in potentiodynamic electrochemical impedance spectroscopy," in *Progress in Chemometrics Research*, A. L. Pomerantsev, Ed., pp. 89–102, Nova Science Publishers, New York, 2005, <http://www.abc.chemistry.bsu.by/vi/analyser/>.
- [18] O. S. Yadav, R. Chaudhary, and A. Gupta, "Synthesis of green inhibitor for mild steel corrosion in a sulphuric acid medium," *Portugaliae Electrochim. Acta.*, vol. 42, no. 5, pp. 355–373, 2024.
- [19] A. Kokalj, "Corrosion inhibitors: physisorbed or chemisorbed?," *Corrosion Science.*, vol. 196, article 109939, 2022.